

# Flowing cryogenic liquid target for terahertz wave generation

Cite as: AIP Advances **10**, 105119 (2020); <https://doi.org/10.1063/5.0023106>

Submitted: 08 September 2020 . Accepted: 28 September 2020 . Published Online: 09 October 2020

Yiwen E , Yuqi Cao, Fang Ling, and X.-C. Zhang 



View Online



Export Citation



CrossMark

## ARTICLES YOU MAY BE INTERESTED IN

[Broadband terahertz wave emission from liquid metal](#)

Applied Physics Letters **117**, 041107 (2020); <https://doi.org/10.1063/5.0015507>

[Impact of the confinement plate on the synthetic jet](#)

AIP Advances **10**, 105204 (2020); <https://doi.org/10.1063/5.0022813>

[Temperature dependent optical and dielectric properties of liquid water studied by terahertz time-domain spectroscopy](#)

AIP Advances **9**, 035346 (2019); <https://doi.org/10.1063/1.5082841>

AIP Advances Nanoscience Collection

READ NOW!

# Flowing cryogenic liquid target for terahertz wave generation

Cite as: AIP Advances 10, 105119 (2020); doi: 10.1063/5.0023106  
Submitted: 8 September 2020 • Accepted: 28 September 2020 •  
Published Online: 9 October 2020



Yiwen E,<sup>1</sup>  Yuqi Cao,<sup>1,2</sup> Fang Ling,<sup>1,3</sup> and X.-C. Zhang<sup>1,a)</sup> 

## AFFILIATIONS

<sup>1</sup>The Institute of Optics, University of Rochester, Rochester, New York 14627, USA

<sup>2</sup>College of Control Science and Engineering, Zhejiang University, Hangzhou 310027, China

<sup>3</sup>College of Electronics and Information Engineering, Sichuan University, Chengdu 610065, China

<sup>a)</sup> Author to whom correspondence should be addressed: [xi-cheng.zhang@rochester.edu](mailto:xi-cheng.zhang@rochester.edu)

## ABSTRACT

Terahertz wave emission from liquids excited by intense laser pulses not only reflects the details in laser–matter interaction but also offers bright terahertz wave sources. Flowing liquid targets possess the advantage of providing a fresh area for each laser pulse. To demonstrate a debris-free target under laser excitation, we investigate the use of liquid nitrogen as a target. By creating a flowing liquid nitrogen line in an ambient environment, we successfully observe broadband terahertz wave emission under short pulse excitation. Our cryogenic line is able to sustain the excitation of a high-repetition-rate (1 kHz) laser. The terahertz peak field emitted from liquid nitrogen is comparable to that from liquid water, yet a broader bandwidth is observed. This demonstration prompts opportunities in choosing potential materials for studying terahertz wave generation processes and in understanding laser-induced ionization of different liquids.

© 2020 Author(s). All article content, except where otherwise noted, is licensed under a Creative Commons Attribution (CC BY) license (<http://creativecommons.org/licenses/by/4.0/>). <https://doi.org/10.1063/5.0023106>

The rapid development of advanced laser technology provides great opportunities to study nonlinear processes in laser–matter interaction. In the terahertz (THz) regime, there is an increasing demand for intense THz sources to enable fundamental studies in ultrafast phenomena,<sup>1–3</sup> such as hidden phase transition,<sup>4</sup> high harmonic generation,<sup>5</sup> and alignment and orientation of molecules.<sup>6</sup> Currently, a THz field over MV/cm is attainable by employing nonlinear crystals.<sup>7,8</sup> Further improvement is limited by the optical damage under intense laser irradiation. Additionally, THz pulse energy above 50 mJ has been reported, with a solid metal target under single-shot excitation by an intense laser pulse (60 J).<sup>9</sup> However, because of the contamination issue caused by debris as well as target damage, solid targets are hardly applied to lasers with a high repetition rate (1 kHz). Therefore, developing a durable target is imperative to provide a solution for intense lasers. Liquid targets with a density similar to that of solid targets are potential candidates due to their capability of providing a fresh area for each pulse. Moreover, liquid targets have been studied for decades in generating extreme ultraviolet and x-ray radiation.<sup>10,11</sup>

Since the first observation of THz waves generated from liquid water,<sup>12,13</sup> more experiments and discussions based on liquid targets

for THz wave generation have been reported. Remarkably, THz field strength up to 0.2 MV/cm has been demonstrated by using a 200  $\mu\text{m}$  water line as the target.<sup>14</sup> The broadband THz wave generated from liquid metal has also been observed.<sup>15</sup> Moreover, the enhancement of THz wave emission induced by a pre-existing plasma in a double-pump excitation geometry is studied to reveal more details in laser–liquid interaction.<sup>16,17</sup> In contrast to an air plasma, the preference for subpicosecond excitation pulses suggests a different ionization process in liquids, in which collisional ionization plays an important role in increasing the electron density.<sup>18</sup> On the other hand, unlike a solid target, the fluidity of liquids can support a continued operation without interruption. Nevertheless, there is still debris when laser intensity is high enough to create a “mist” from the target, which not only contaminates the optics nearby but also absorbs and scatters the signal. It should be noted that while gas is a good debris-free target, it hardly supports a high-density plasma because of the relatively low molecular density.

To demonstrate a debris-free target for THz wave emission, we create a free-standing, flowing liquid nitrogen (LN<sub>2</sub>) line in an ambient environment. Applying single color excitation, coherent THz emission is detected in the forward direction by electro-optic

sampling (EOS). Compared with the signal from liquid water under the same excitation condition, the signal from LN<sub>2</sub> has a comparable peak field but a broader bandwidth, which is attributed to the low absorption of LN<sub>2</sub> at higher THz frequency. The LN<sub>2</sub> target can support the excitation by laser pulses with a 1 kHz repetition rate without interruption.

Figure 1(a) shows the apparatus for creating a gravity-driving, free-standing liquid line of LN<sub>2</sub>. It consists of a syringe, a flask, and an insulating layer. Specifically, a metal syringe is used for guiding the flow of liquid nitrogen, and it is immersed in a flask filled with LN<sub>2</sub> for maintaining the cryogenic temperature. Outside the flask, a thick insulating layer is employed to resist the heat transition between the flask and the ambient environment. The volume of the flask is 600 ml. While filling the flask with LN<sub>2</sub>, the syringe is blocked on purpose at the beginning until the setup is cooled down. Benefiting from the high thermal conductivity of the metal syringe, the setup reaches a thermal balance in a few minutes. After removing the block, a small amount of vaporized nitrogen gas is first ejected out from the syringe needle. Then, a steady liquid line is formed.

Figure 1(b) (multimedia view) shows a photo taken by a CCD camera showing the flowing LN<sub>2</sub> line. The inner diameter of the syringe needle is about 410 μm. From the photo, the diameter of the flow is estimated to be 400 ± 5 μm. The liquid line shows high transparency, indicating a smooth surface and a stable flow. In addition, a 10-s video clearly shows the flowing LN<sub>2</sub> line and its stability. For comparison, Fig. 1(c) shows the ejection of a gas-liquid mixture when the flask is connected to a Dewar directly. The pressure difference inside and outside the Dewar results in a different boiling point, which causes transient vaporization when LN<sub>2</sub> ejects out. The all-white color indicates a strong scattering. To get rid of the gas phase, a phase separator is used between the Dewar and the flask.

As a target, the surface smoothness and stability of the flow are key to getting a good signal-to-noise ratio. In fluid mechanics, a flowing liquid can be characterized by the Reynolds number ( $Re$ ),<sup>19</sup> which is a dimensionless quantity, defined as

$$Re = \frac{2\rho vr}{\eta}, \quad (1)$$

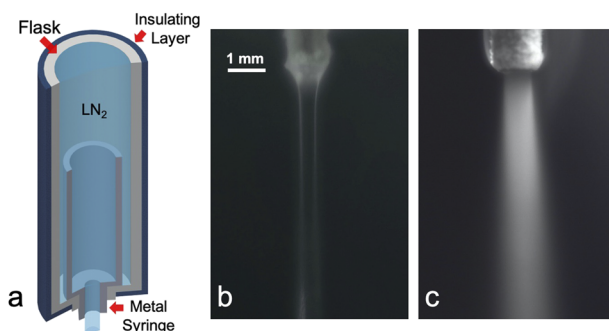


FIG. 1. (a) Diagram of the apparatus for guiding an LN<sub>2</sub> line, (b) the photo of a flowing LN<sub>2</sub> line in an ambient environment (a 10-s video is also provided to show its stability), and (c) the photo of a mixture of gas and liquid nitrogen. Multimedia view: (b): <https://doi.org/10.1063/5.0023106.1>

where  $\rho$ ,  $v$ ,  $r$ , and  $\eta$  are the density (g/cm<sup>3</sup>), flow rate (m/s), radius (m), and dynamic viscosity ( $\mu$ Pa s) of the liquid, respectively.  $Re$  shows the ratio between the inertial force to the viscous force. When  $Re < 2300$ , laminar flow is formed with no lateral mixing or turbulence,<sup>20</sup> in which the liquid is regarded as several layers moving smoothly. Laminar flow offers a good-quality target for optical excitation. From Eq. (1), we know that a low flow rate and a high viscosity are in favor of small  $Re$ . However, as a target designed for a laser with a 1 kHz repetition rate, the flow rate ( $v$ ) needs to be greater than 1 m/s to provide each pulse a fresh area. LN<sub>2</sub> has a relatively low viscosity ( $\eta = 150 \mu$ Pa s at 77 K), leading to difficulty in creating a Laminar flow. In our case, to avoid a turbulent flow,  $Re$  is kept at 2150 by selecting the syringe with an appropriate diameter.

It should be noted that the LN<sub>2</sub> line is flowing in the ambient environment. This is possible because of the Leidenfrost effect,<sup>21,22</sup> in which an insulating layer is created at the surface by the vaporized LN<sub>2</sub> to keep the liquid from boiling rapidly. The liquid line will break into droplets eventually due to surface energy minimization. The break-up distance  $L$  from the needle tip can be calculated by<sup>23</sup>

$$L = 12v \left( \sqrt{\frac{8\rho r^3}{\sigma} + \frac{6\eta r}{\sigma}} \right), \quad (2)$$

wherein  $\sigma$  is the surface tension. For LN<sub>2</sub> at 77 K,  $\sigma$  is 8.94 mN/m.  $L = 29$  mm is calculated in our case. Before breaking into droplets, the surface smoothness and stability decrease with the distance from the needle tip.

In the optical excitation setup, laser pulses with an 800 nm central wavelength (370 fs, 0.4 mJ) are focused into the LN<sub>2</sub> target. With a lens of 2-in. focal length, the beam waist is about 2.6 μm. The focus position is about 2 mm away from the tip of the syringe needle, which is in the area of a cylindrical line with a smooth surface and far away from droplets. THz waveforms are measured in the forward direction by EOS with a 2-mm thick ZnTe crystal. More details of the experimental setup can be found in Ref. 12.

The normalized THz waveforms from an LN<sub>2</sub> line and a water line under the same experimental conditions are shown in Fig. 2.

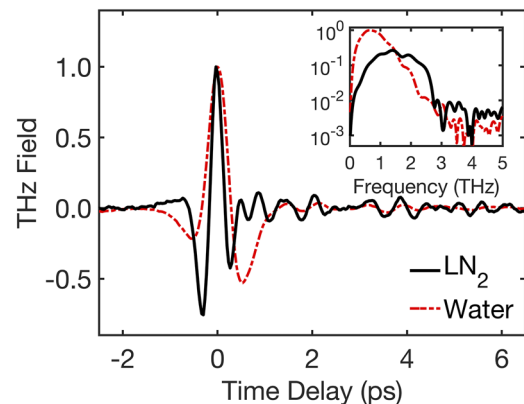
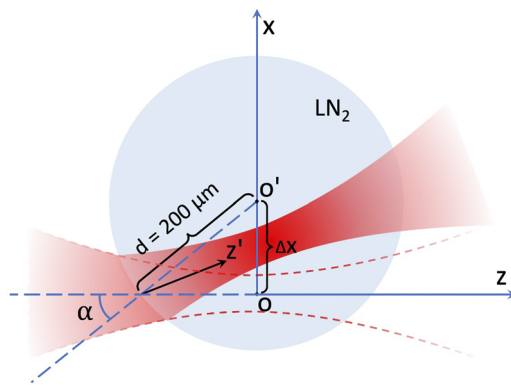


FIG. 2. Detected THz waveforms from a water line (210 μm) and an LN<sub>2</sub> line (400 μm). The corresponding spectra are shown in the inset. The LN<sub>2</sub> signal shows a narrower pulse duration, and its spectrum has a broader bandwidth.



**FIG. 3.** Cross section of the liquid line to show the relative position of the LN<sub>2</sub> line and the focused laser beam. Laser propagates in the  $z$  direction (red dash line). The incident angle  $\alpha$  continuously changes by scanning the LN<sub>2</sub> line in the  $x$  direction, in which  $\alpha = \arcsin(\Delta x/r)$ , where  $\Delta x$  is the distance of the liquid centroid away from the  $z$  direction,  $r$  is the radius of the liquid line, and  $z'$  is the direction of the refracted laser beam at the air/liquid surface.

Currently, the peak field from LN<sub>2</sub> is 0.4 times weaker than that from water. However, the THz signal from LN<sub>2</sub> shows a shorter pulse duration. By fitting the envelope of the signal in the field, the waveform from LN<sub>2</sub> has a pulse duration of 0.6 ps. The corresponding spectra without normalization are shown in the inset for comparing the real magnitude between two signals. Under the same excitation and detection conditions, the LN<sub>2</sub> shows a broader bandwidth with more high-frequency components. There are two possible reasons. First, LN<sub>2</sub> has a low absorption in THz frequency because it is a nonpolar liquid.<sup>24</sup> Additionally, the vaporized N<sub>2</sub> keeps purging the system to preserve the high frequency components. The cutoff frequency is about 2.5 THz, which is limited by the detection crystal. THz wave emission from bulk LN<sub>2</sub> under a two-color or double pump excitation was recently reported,<sup>25</sup> in which a bolometer is used for detection. Distinctively, we are using a flowing LN<sub>2</sub> line and measuring a temporal THz waveform.

The THz wave emission from liquids is extremely sensitive to the position of the liquid target across the focus. Figure 3 shows the cross section of a liquid line and the laser beam. By scanning the position of the LN<sub>2</sub> line in the  $x$  direction from  $x = 0$ , the incidence angle ( $\alpha$ ) at the air/liquid interface is continuously increasing from  $0^\circ$  to  $90^\circ$ , which can be calculated by  $\alpha = \arcsin(\Delta x/r)$ . Here,  $\Delta x$  is the distance of the liquid centroid away from the  $z$  axis. The direction of the dipole created by the ponderomotive force is along the laser propagating direction. The laser beam refracts at the air/liquid interface, leading to a deviation of the dipole from the  $z$  direction. As it has been discussed in our previous work,<sup>26</sup> there is an optimized incidence angle to get the maximal THz field coupled out from the liquid, which is determined by the dipole projection in the direction of detection and the total internal reflection of the THz wave at the liquid/air interface. Here, the projection in the  $x$ -axis mainly contributes to the signal we measured.

Figure 4(a) plots the dependence of THz peak field on the  $x$ -position of the liquid line. By moving the target from the negative to the positive direction, the electric field has an opposite sign. The maximized signal is obtained at  $\Delta x = \pm 170 \mu\text{m}$ , showing that the

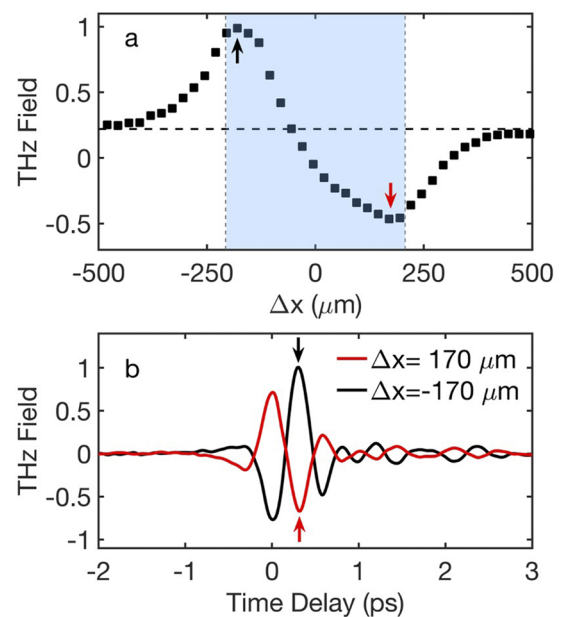


**FIG. 4.** (a) Dependence of THz field strength on the liquid line position when the time delay is 0.3 ps. The blue shadow shows the diameter of the liquid line. The baseline offset shows the amplitude of the THz signal from air plasma under the same excitation condition and (b) flipped THz waveforms when  $\Delta x = -170 \mu\text{m}$  and  $170 \mu\text{m}$ . The corresponding positions are labeled by arrows in plot (a). The incidence angle  $|\alpha| = 50.6^\circ$  when  $\Delta x = \pm 170 \mu\text{m}$ .

optimal incidence angle is  $50.6^\circ$ . As a nonpolar liquid, LN<sub>2</sub> has a much lower absorption coefficient ( $0.8 \text{ cm}^{-1}$  near 1 THz)<sup>24</sup> than that of water ( $220 \text{ cm}^{-1}$  near 1 THz).<sup>27</sup> A lower refractive index is expected, which results in a smaller optimal incidence angle. For the laser beam, the difference in the refractive index between liquid water (1.3) and LN<sub>2</sub> (1.2) is too small to be a dominant factor here. The baseline offset shown in Fig. 4(a) is the amplitude of THz emission from air plasma when the liquid target is moved away from the laser focus. Then, the field amplitude gradually increases when the liquid line is moved toward the focus. It can be explained that the molecular density near the liquid line gradually increased by the vaporization of LN<sub>2</sub>. Additionally, the result clearly shows that under the excitation of sub-picosecond pulse, the signal from a liquid is stronger than that from air.

Figure 4(b) shows the waveforms when  $\Delta x = \pm 170 \mu\text{m}$ . The waveforms have the same shape with an opposite polarity. This is because the dipole projection in the  $x$  direction has an opposite direction, which clearly indicates that the THz signal is from a liquid phase rather than a vaporized gas phase. This demonstration also shows that the flowing liquid target can be applied to both normal and cryogenic liquid. Moreover, flowing liquid nitrogen is a debris-free target, and the mist is vaporized immediately without contamination and scattering.

Currently, THz wave generation from liquids under single-color excitation can be explained by the ponderomotive force-induced dipole.<sup>14,26</sup> However, many properties remain unclear, namely, which properties of liquids can lead to a high field and

a broad bandwidth? Two nonpolar liquids have been tested,  $\alpha$ -pinene<sup>16</sup> and liquid nitrogen (in this paper). Both of them provide a broader bandwidth of THz signals than that from water, which suggests the significance of the low absorption. On the other hand, a much brighter white light from liquids than that from air plasma is observed in the experiment, which indicates that the liquid does provide more electrons in the ionization process. The relationship between ionized electrons and generation efficiency needs to be studied further.

In summary, we report a temporal THz waveform from a flowing cryogenic line under single-color excitation. Compared to the THz signal from liquid water, a comparable electric field but with a broader bandwidth is observed. Our results show that LN<sub>2</sub> has the potential to be a THz source for generating broadband THz pulses without producing debris. Furthermore, ionized LN<sub>2</sub> can also emit x-rays. Along with THz rays, they are able to reflect different dynamics of ionized electrons. Detecting two synchronized pulses (x-rays and THz rays) as well as the white light in the same ionization process is meaningful to portray a full picture of electron dynamics from excitation to recombination. In addition, developing a flowing liquid target (line/droplets) for high repetition rate lasers will facilitate studies of laser-liquid interaction in diverse materials.

The research at the University of Rochester was sponsored by the Army Research Office, under Grant No. W911NF-17-1-0428, the Air Force Office of Scientific Research, under Grant No. FA9550-18-1-0357, and the National Science Foundation, under Grant No. ECCS-1916068.

## DATA AVAILABILITY

The data that support the findings of this study are available from the corresponding author upon reasonable request.

## REFERENCES

- <sup>1</sup>H. A. Hafez, S. Kovalev, K. J. Tielrooij, M. Bonn, M. Gensch, and D. Turchinovich, *Adv. Opt. Mater.* **8**(3), 1900771 (2020).
- <sup>2</sup>X. C. Zhang, A. Shkurinov, and Y. Zhang, *Nat. Photonics* **11**(1), 16 (2017).
- <sup>3</sup>T. Kampfrath, K. Tanaka, and K. A. Nelson, *Nat. Photonics* **7**(9), 680 (2013).
- <sup>4</sup>X. Li, T. Qiu, J. Zhang, E. Baldini, J. Lu, A. M. Rappe, and K. A. Nelson, *Science* **364**(6445), 1079 (2019).
- <sup>5</sup>H. A. Hafez, S. Kovalev, J.-C. Deinert, Z. Mics, B. Green, N. Awari, M. Chen, S. Germanskiy, U. Lehnert, J. Teichert *et al.*, *Nature* **561**(7724), 507 (2018).
- <sup>6</sup>S. Fleischer, Y. Zhou, R. W. Field, and K. A. Nelson, *Phys. Rev. Lett.* **107**(16), 163603 (2011).
- <sup>7</sup>H. Hirori, A. Doi, F. Blanchard, and K. Tanaka, *Appl. Phys. Lett.* **98**(9), 091106 (2011).
- <sup>8</sup>C. P. Hauri, C. Ruchert, C. Vicario, and F. Ardana, *Appl. Phys. Lett.* **99**(16), 161116 (2011).
- <sup>9</sup>G. Liao, Y. Li, H. Liu, G. G. Scott, D. Neely, Y. Zhang, B. Zhu, Z. Zhang, C. Armstrong, E. Zemaityte, P. Bradford, P. G. Huggard, D. R. Rusby, P. McKenna, C. M. Brenner, N. C. Woolsey, W. Wang, Z. Sheng, and J. Zhang, *Proc. Natl. Acad. Sci. U. S. A.* **116**(10), 3994 (2019).
- <sup>10</sup>L. Malmqvist, L. Rymell, M. Berglund, and H. M. Hertz, *Rev. Sci. Instrum.* **67**(12), 4150 (1996).
- <sup>11</sup>K. M. George, J. T. Morrison, S. Feister, G. K. Ngirang, J. R. Smith, A. J. Klim, J. Snyder, D. Austin, W. Erbsen, K. D. Frische *et al.*, *High Power Laser Sci. Eng.* **7**, e50 (2019).
- <sup>12</sup>Q. Jin, Y. E. K. Williams, J. Dai, and X.-C. Zhang, *Appl. Phys. Lett.* **111**(7), 071103 (2017).
- <sup>13</sup>I. Dey, K. Jana, V. Yu Fedorov, A. D. Koulouklidis, A. Mondal, M. Shaikh, D. Sarkar, A. D. Lad, S. Tzortzakakis, A. Couairon *et al.*, *Nat. Commun.* **8**(1), 1184 (2017).
- <sup>14</sup>L.-L. Zhang, W.-M. Wang, T. Wu, S.-J. Feng, K. Kang, C.-L. Zhang, Y. Zhang, Y.-T. Li, Z.-M. Sheng, and X.-C. Zhang, *Phys. Rev. Appl.* **12**(1), 014005 (2019).
- <sup>15</sup>Y. Cao, E. Yiwen, P. Huang, and X.-C. Zhang, *Appl. Phys. Lett.* **117**(4), 041107 (2020).
- <sup>16</sup>E. Yiwen, Q. Jin, and X.-C. Zhang, *Appl. Phys. Lett.* **115**, 101101 (2019).
- <sup>17</sup>E. A. Ponomareva, A. N. Tcypkin, S. V. Smirnov, S. E. Putilin, E. Yiwen, S. A. Kozlov, and X.-C. Zhang, *Opt. Express* **27**(22), 32855 (2019).
- <sup>18</sup>Q. Jin, E. Yiwen, S. Gao, and X.-C. Zhang, *Adv. Photonics* **2**(1), 015001 (2020).
- <sup>19</sup>O. Reynolds, *Philos. Trans. R. Soc. London* **174**, 935 (1883).
- <sup>20</sup>A. D. Kraus, R. W. James, and A. Aziz, *Introduction to Thermal and Fluid Engineering* (CRC Press, 2011).
- <sup>21</sup>J. G. Leidenfrost, *De Aquae Communis Nonnullis Qualitatibus Tractatus* (Ovenius, 1756).
- <sup>22</sup>B. S. Gottfried, C. J. Lee, and K. J. Bell, *Int. J. Heat Mass Transfer* **9**(11), 1167 (1966).
- <sup>23</sup>M. J. McCarthy and N. A. Molloy, *Chem. Eng. J.* **7**(1), 1 (1974).
- <sup>24</sup>J. Samios, U. Mittag, and T. Dorfmueller, *Mol. Phys.* **56**(3), 541 (1985).
- <sup>25</sup>A. V. Balakin, J.-L. Coutaz, V. A. Makarov, I. A. Kotelnikov, Y. Peng, P. M. Solyankin, Y. Zhu, and A. P. Shkurinov, *Photonics Res.* **7**(6), 678 (2019).
- <sup>26</sup>E. Yiwen, Q. Jin, A. Tcypkin, and X.-C. Zhang, *Appl. Phys. Lett.* **113**, 181103 (2018).
- <sup>27</sup>T. Wang, P. Klarskov, and P. U. Jepsen, *IEEE Trans. Terahertz Sci. Technol.* **4**(4), 425 (2014).